

## Strongly enhanced effective mass in dilute two-dimensional electron systems: System-independent origin

A. A. Shashkin, A. A. Kapustin, E. V. Deviatov, and V. T. Dolgoplov  
*Institute of Solid State Physics, Chernogolovka, Moscow District 142432, Russia*

Z. D. Kvon  
*Institute of Semiconductor Physics, Novosibirsk, Russia*  
(Received 14 November 2007; published 10 December 2007)

We measure the effective mass in a dilute two-dimensional electron system in (111) silicon by analyzing the temperature dependence of the Shubnikov–de Haas oscillations in the low-temperature limit. A strong enhancement of the effective mass with decreasing electron density is observed. The mass renormalization as a function of the interaction parameter  $r_s$  is in good agreement with that reported for (100) silicon, which shows that the relative mass enhancement is system and disorder independent, being determined by electron-electron interactions only.

DOI: [10.1103/PhysRevB.76.241302](https://doi.org/10.1103/PhysRevB.76.241302)

PACS number(s): 73.40.Qv, 71.30.+h, 71.18.+y

The ground state of an ideal, strongly interacting two-dimensional (2D) electron system is expected to be a Wigner crystal.<sup>1</sup> The interaction strength is characterized by the Wigner-Seitz radius  $r_s$ , which is equal in the single-valley case to the ratio between the Coulomb energy and the Fermi energy,  $E_C/E_F$ . This ratio is proportional to  $n_s^{-1/2}$  and therefore increases with decreasing electron density  $n_s$ . According to numerical simulations,<sup>2</sup> Wigner crystallization is expected at  $r_s \approx 35$ . The refined numerical simulations<sup>3</sup> have predicted that, prior to the crystallization, in the range of the interaction parameter  $25 \lesssim r_s \lesssim 35$ , the ground state of the system is a strongly correlated ferromagnetic Fermi liquid; yet other intermediate phases may also exist.<sup>4</sup> At  $r_s \sim 1$ , the electron liquid is expected to be paramagnetic, with the effective mass  $m$  and Landé  $g$  factor renormalized by interactions. It was not until recently that qualitative deviations from the weakly interacting Fermi liquid behavior (in particular, the drastic increase of the effective electron mass with decreasing electron density) were found in strongly correlated 2D electron systems ( $r_s \geq 10$ ).<sup>5–7</sup>

The strongest many-body effects have been observed in (100) silicon metal-oxide-semiconductor field-effect transistors (MOSFETs). Due to this, there has been recently a revival of interest to (111) silicon MOSFETs.<sup>8–10</sup> Although the latter electron system has been under study for quite a long time, the main experimental results were obtained some decades ago (see, e.g., Ref. 11), when the knowledge of 2D electron systems left much to be desired. The electron densities and temperatures used in experiments were not low enough and the experimental accuracy achieved for low-mobility samples was not high enough.

In this paper, we report accurate measurements of the effective mass in a dilute 2D electron system in (111) silicon by analyzing temperature dependence of the weak-field Shubnikov–de Haas (SdH) oscillations in the low-temperature limit. We find that the effective mass is strongly increased at low electron densities. The renormalization of the effective mass as a function of the interaction parameter  $r_s$  agrees well with that found in (100) silicon MOSFETs, although the effective masses in bulk silicon for both orien-

tations are different by a factor of about 2. Also, our (111) samples have a much higher level of disorder than (100) samples. This gives evidence that the relative mass enhancement is system and disorder independent and is determined by electron-electron interactions only.

Measurements were made in an Oxford dilution refrigerator with a base temperature of  $\approx 30$  mK on (111) silicon MOSFETs similar to those previously used in Ref. 8. Samples had the Hall bar geometry with width  $400 \mu\text{m}$  equal to the distance between the potential probes. Application of a dc voltage to the gate relative to the contacts allowed control of the electron density. The oxide thickness was equal to  $1540 \text{ \AA}$ . In the highest-mobility samples, the normal of the sample surface was tilted from  $[111]$  toward the  $[110]$  direction by a small angle of  $8^\circ$ . Anisotropy for electron transport in such samples does not exceed 5% at  $n_s = 3 \times 10^{11} \text{ cm}^{-2}$  and increases weakly with electron density, staying below 25% at  $n_s = 3 \times 10^{12} \text{ cm}^{-2}$ , as has been determined in independent experiments. The resistance  $R_{xx}$  was measured by a standard four-terminal technique at a low frequency (5–11 Hz) to minimize the out-of-phase signal. The excitation current was kept low enough (3–40 nA) to ensure that measurements were taken in the linear regime of response. SdH oscillations were studied on two samples, and very similar results were obtained. In particular, the extracted values of the effective mass were coincident within our experimental uncertainty. Below, we show results obtained on a sample with a peak electron mobility close to  $2500 \text{ cm}^2/\text{V s}$  at  $T = 1.5 \text{ K}$ .

In Fig. 1(a), we show the magnetoresistance  $R_{xx}(B)$  for  $n_s = 8.4 \times 10^{11} \text{ cm}^{-2}$  at different temperatures. In weak magnetic fields, the SdH oscillation period corresponds to a change of the filling factor  $\nu = n_s hc/eB$  by  $\Delta\nu = 4$ ,<sup>12</sup> which indicates that both the spin and valley degeneracies are equal to  $g_s = g_v = 2$ . The fact that the valley degeneracy is equal to  $g_v = 2$ , rather than  $g_v = 6$ , is a long-standing problem which lacks a definite answer so far.<sup>8</sup>

In Fig. 1(b), we plot the positions of the resistance minima in the  $(B, n_s)$  plane. The symbols are the experimental data and the lines are the expected positions of the cyclotron and spin minima calculated according to the formula

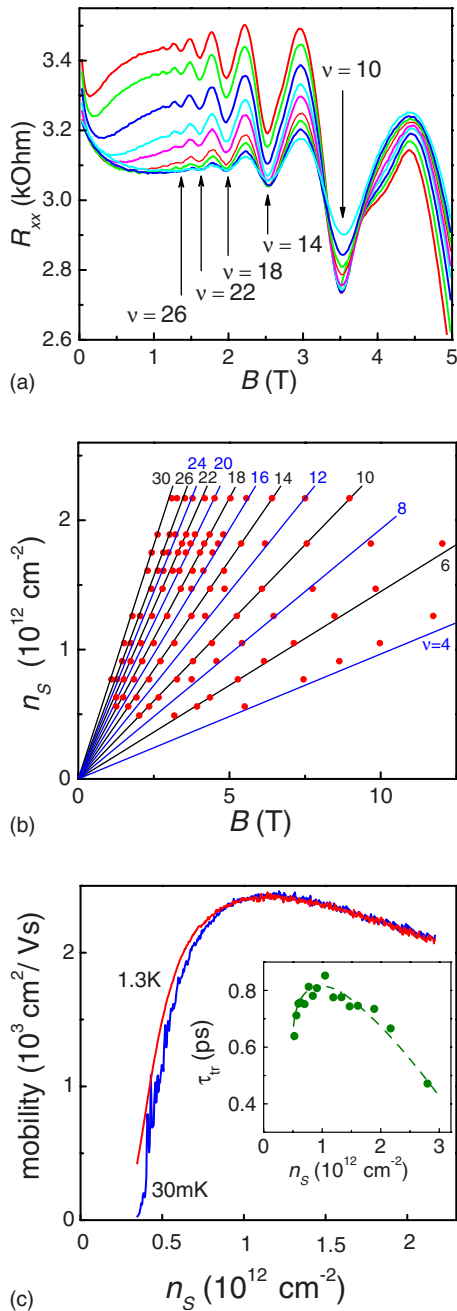


FIG. 1. (Color online) (a) Shubnikov–de Haas oscillations in the (111) Si MOSFET at  $n_s = 8.4 \times 10^{11} \text{ cm}^{-2}$  for the following temperatures (from top to bottom): 0.03, 0.12, 0.2, 0.3, 0.38, 0.47, 0.55, 0.62, and 0.75 K. (b) Positions of the SdH oscillation minima in the  $(B, n_s)$  plane (dots) and the expected positions of the cyclotron and spin minima calculated according to the formula  $n_s = \nu eB/hc$  (solid lines). (c) Dependence of the zero-field mobility on electron density at different temperatures. Inset: transport scattering time versus  $n_s$  evaluated from zero-field mobility, taking account of the mass renormalization. The dashed line is a guide to the eye.

$n_s = \nu eB/hc$ . Resistance minima are seen at  $\nu = 6, 10, 14, 18, 22, 26,$  and  $30$  corresponding to spin splittings and at  $\nu = 4, 8, 12, 16, 20, 24,$  and  $28$  corresponding to cyclotron gaps. The valley splitting is not seen at low electron densities in weak magnetic fields, and the even numbers of the SdH oscillation

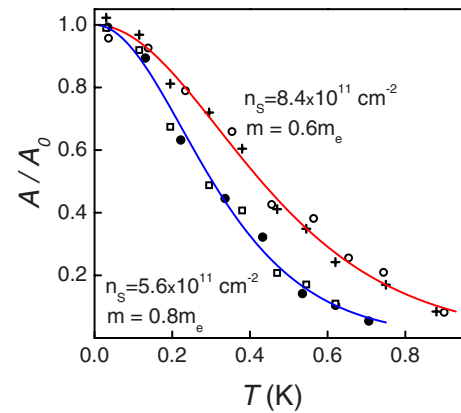


FIG. 2. (Color online) Change of the amplitude of the weak-field SdH oscillations with temperature for magnetic fields  $B_1 = 1.44 \text{ T}$  (dots),  $B_2 = 1.64 \text{ T}$  (squares), and  $B_1 = 1.45 \text{ T}$  (open circles), and  $B_2 = 1.74 \text{ T}$  (crosses). The value of  $T$  for the  $B_1$  data is multiplied by the ratio  $B_2/B_1$ . The solid lines are fits using Eq. (1).

minima confirm the valley degeneracy equal to  $g_v = 2$ . The spin minima extend to appreciably lower electron densities than the cyclotron minima; behavior that is similar to that observed in (100) silicon MOSFETs.<sup>13</sup> This reveals that, at the lowest electron densities, the spin splitting is close to the cyclotron splitting, i.e., the product  $gm$  is strongly enhanced (by a factor of about 3).

We would like to emphasize that, unlike (100) silicon MOSFETs with mobilities in excess of  $\approx 2 \times 10^4 \text{ cm}^2/\text{V s}$ , the metallic temperature dependence of the  $B=0$  resistance is not observed below  $T = 1.3 \text{ K}$  in our samples, as is evident from Fig. 1(c), which shows the zero-field mobility as a function of electron density at different temperatures.

A typical temperature dependence of the amplitude  $A$  of the weak-field (sinusoidal) SdH oscillations for the normalized resistance  $R_{xx}/R_0$  (where  $R_0$  is the average resistance) is displayed in Fig. 2. To determine the effective mass, we use the method of Ref. 14, extending it to low electron densities and temperatures. We fit the data for  $A(T)$  using the formula

$$A(T) = A_0 \frac{2\pi^2 k_B T / \hbar \omega_c}{\sinh(2\pi^2 k_B T / \hbar \omega_c)},$$

$$A_0 = 4 \exp(-2\pi^2 k_B T_D / \hbar \omega_c), \quad (1)$$

where  $\omega_c = eB/mc$  is the cyclotron frequency and  $T_D$  is the Dingle temperature.<sup>15,16</sup> The latter is related to the level width through the expression  $T_D = \hbar / 2\pi k_B \tau$ , where  $\tau$  is the quantum scattering time.<sup>17</sup> In principle, a temperature-dependent  $\tau$  may influence damping of the SdH oscillations with temperature. In our experiment, however, possible corrections to the mass value caused by the temperature dependence of  $\tau$  (and hence  $T_D$ ) are within the experimental uncertainty, which is estimated by data dispersion at about 10%. Note that the amplitude of the SdH oscillations follows the calculated curve down to the lowest achieved temperatures, which confirms that the electrons were in good thermal contact with the bath and were not overheated. The applica-

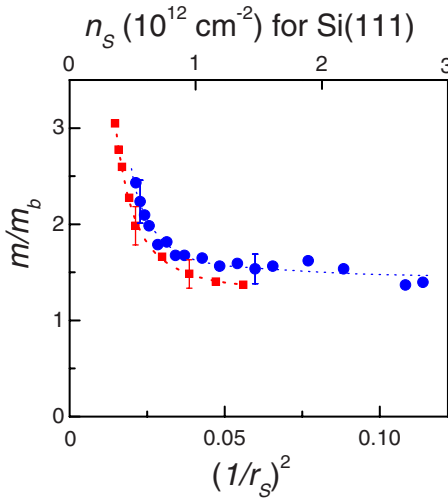


FIG. 3. (Color online) Effective mass (dots) in units of  $m_b$  as a function of  $(1/r_s)^2 \propto n_s$ . Also shown by squares are the data obtained in (100) Si MOSFETs (Ref. 16). The dashed lines are guides to the eye.

bility of Eq. (1) to strongly interacting 2D electron systems is justified by the coincidence of the enhanced mass values obtained in (100) silicon MOSFETs using a number of independent measurement methods including this one.<sup>7,16,18</sup>

In Fig. 3, we show the effective mass so determined in units of the cyclotron mass in bulk silicon,  $m_b = 0.358m_e$  (where  $m_e$  is the free electron mass), as a function of  $(1/r_s)^2 \propto n_s$ . (For the two-valley case the ratio  $E_C/E_F$  that determines the system behavior is twice as large as the Wigner-Seitz radius  $r_s$ . To avoid confusion, below we will still use the Wigner-Seitz radius with the average dielectric constant of 7.7 as the interaction parameter.) The effective mass sharply increases with decreasing electron density, its enhancement at low  $n_s$  being consistent with that of  $gm$ . The mass renormalization  $m/m_b$  versus the interaction parameter  $r_s$  is coincident within the experimental uncertainty with that found in (100) silicon MOSFETs, where  $m_b = 0.19m_e$  is approximately twice as small and the peak mobility is approximately one order of magnitude as large. Thus, we arrive at the conclusion that the relative mass enhancement is determined by  $r_s$ , being independent of the 2D electron system. Note that the highest accessible  $r_s$  is different in different 2D electron systems.

In Fig. 4, we compare the extracted Dingle temperature  $T_D$  with that recalculated from the electron lifetime  $\tau_{tr}$  that is evaluated from the zero-field mobility, taking into account the mass renormalization<sup>18</sup> [inset to Fig. 1(c)]. Although the quantum scattering time  $\tau$  defining the Dingle temperature is in general different from the transport scattering time  $\tau_{tr}$ , the two  $T_D(n_s)$  dependences are consistent with each other at  $(1/r_s)^2 > 0.04$ , indicating dominant large-angle scattering.<sup>17</sup> The measured value of  $T_D$  at the same  $r_s$  is considerably larger in (111) silicon than in (100) silicon MOSFETs and, therefore, the Dingle temperature increases with disorder. In both electron systems, the Dingle temperature decreases with decreasing electron density. It is worth noting that the different behavior of the measured and recalculated  $T_D(n_s)$  depen-

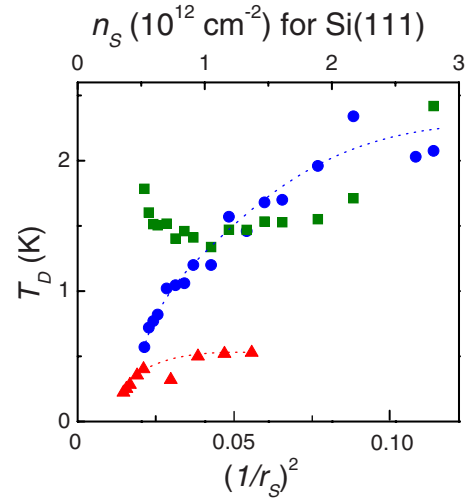


FIG. 4. (Color online) Behavior of the Dingle temperature extracted from SdH oscillations (dots) and that calculated from the transport scattering time (squares) with  $(1/r_s)^2 \propto n_s$ . Also shown by triangles is the data obtained from SdH oscillations in (100) Si MOSFETs (Ref. 16). The dashed lines are guides to the eye.

dences at low electron densities [at  $(1/r_s)^2 < 0.04$ ] is consistent with predictions of the scattering theory of Ref. 19. There, it was shown that multiple scattering effects lead to a decrease of the ratio  $\tau_{tr}/\tau$  at low electron densities so that this ratio tends to zero at the metal-insulator transition.

We now discuss the results obtained for the effective mass. We stress that a strongly increased mass is observed in a dilute 2D electron system with relatively high disorder, as inferred from both the relatively low zero-field mobility and the absence of metallic temperature dependence of the zero-field resistance. Moreover, the disorder does not at all influence the relative enhancement of the mass as a function of the interaction parameter. This allows us to claim that the mass enhancement is solely caused by electron-electron interactions. Our results also add confidence that the dilute system behavior in the regime of strongly enhanced spin susceptibility  $\chi \propto gm$ —close to the onset of spontaneous spin polarization and Wigner crystallization—is governed by the effective mass.

The finding that in dilute 2D electron systems the effective mass is strongly enhanced remains basically unexplained, although there has been a good deal of theoretical work on the subject (see Refs. 5 and 20 and references therein). The latest theoretical developments include the following. Using a renormalization group analysis for multivalley 2D systems, it has been found that the effective mass dramatically increases at a disorder-dependent density for the metal-insulator transition, while the  $g$  factor remains nearly intact.<sup>21</sup> However, the prediction of disorder-dependent effective mass is not confirmed by our data. In the Fermi-liquid-based model of Ref. 22, a flattening at the Fermi energy in the spectrum that leads to a diverging effective mass was predicted. Still, the expected dependence of the effective mass on temperature is not consistent with experimental findings.

Finally, we would like to note that moderate enhance-

ments of the effective mass  $m \approx 1.5m_b$  have been determined in 2D electron systems of AlAs quantum wells and GaAs/AlGaAs heterostructures because the lowest accessible densities are still too high.<sup>23–25</sup> While the theories of, e.g., Refs. 26 and 27 are capable of describing the experimental  $m(n_s)$  dependence at  $r_s \sim 1$ , their validity at larger values of the interaction parameter is a problem.

In summary, we have found that in a dilute 2D electron system in (111) silicon, the effective mass sharply increases at low electron densities. The mass renormalization versus the interaction parameter  $r_s$  is in good agreement with that reported for (100) silicon MOSFETs. This gives evidence

that the relative mass enhancement is system and disorder independent and is solely determined by electron-electron interactions. The results obtained show that the dilute system behavior in the regime of the strongly enhanced spin susceptibility is governed by the effective mass. The particular mechanism underlying the effective mass enhancement remains to be seen.

We gratefully acknowledge discussions with E. Abrahams, A. Gold, S. V. Kravchenko, and A. Punnoose. This work was supported by the RFBR, RAS, and the program “The State Support of Leading Scientific Schools.”

- 
- <sup>1</sup>E. Wigner, Phys. Rev. **46**, 1002 (1934).  
<sup>2</sup>B. Tanatar and D. M. Ceperley, Phys. Rev. B **39**, 5005 (1989).  
<sup>3</sup>C. Attaccalite, S. Moroni, P. Gori-Giorgi, and G. B. Bachelet, Phys. Rev. Lett. **88**, 256601 (2002).  
<sup>4</sup>B. Spivak, Phys. Rev. B **67**, 125205 (2003).  
<sup>5</sup>S. V. Kravchenko and M. P. Sarachik, Rep. Prog. Phys. **67**, 1 (2004); A. A. Shashkin, Phys. Usp. **48**, 129 (2005).  
<sup>6</sup>A. A. Shashkin, S. Anissimova, M. R. Sakr, S. V. Kravchenko, V. T. Dolgoplov, and T. M. Klapwijk, Phys. Rev. Lett. **96**, 036403 (2006).  
<sup>7</sup>S. Anissimova, A. Venkatesan, A. A. Shashkin, M. R. Sakr, S. V. Kravchenko, and T. M. Klapwijk, Phys. Rev. Lett. **96**, 046409 (2006).  
<sup>8</sup>O. Estibals, Z. D. Kvon, G. M. Gusev, G. Arnaud, and J. C. Portal, Physica E (Amsterdam) **22**, 446 (2004).  
<sup>9</sup>K. Eng, R. N. McFarland, and B. E. Kane, Appl. Phys. Lett. **87**, 052106 (2005); Physica E (Amsterdam) **34**, 701 (2006).  
<sup>10</sup>K. Eng, R. N. McFarland, and B. E. Kane, Phys. Rev. Lett. **99**, 016801 (2007).  
<sup>11</sup>T. Neugebauer, K. v. Klitzing, G. Landwehr, and G. Dorda, Solid State Commun. **17**, 295 (1975).  
<sup>12</sup>On the higher-mobility Si(111) samples of Ref. 10, a periodicity  $\Delta\nu=8$  was observed in weak magnetic fields.  
<sup>13</sup>S. V. Kravchenko, A. A. Shashkin, D. A. Bloore, and T. M. Klapwijk, Solid State Commun. **116**, 495 (2000).  
<sup>14</sup>J. L. Smith and P. J. Stiles, Phys. Rev. Lett. **29**, 102 (1972).  
<sup>15</sup>I. M. Lifshitz and A. M. Kosevich, Zh. Eksp. Teor. Fiz. **29**, 730 (1955); A. Isihara and L. Smrcka, J. Phys. C **19**, 6777 (1986).  
<sup>16</sup>A. A. Shashkin, M. Rahimi, S. Anissimova, S. V. Kravchenko, V. T. Dolgoplov, and T. M. Klapwijk, Phys. Rev. Lett. **91**, 046403 (2003).  
<sup>17</sup>T. Ando, A. B. Fowler, and F. Stern, Rev. Mod. Phys. **54**, 437 (1982).  
<sup>18</sup>A. A. Shashkin, S. V. Kravchenko, V. T. Dolgoplov, and T. M. Klapwijk, Phys. Rev. B **66**, 073303 (2002).  
<sup>19</sup>A. Gold, Phys. Rev. B **38**, 10798 (1988).  
<sup>20</sup>S. V. Kravchenko, A. A. Shashkin, S. Anissimova, A. Venkatesan, M. R. Sakr, V. T. Dolgoplov, and T. M. Klapwijk, Ann. Phys. (N.Y.) **321**, 1588 (2006).  
<sup>21</sup>A. Punnoose and A. M. Finkelstein, Science **310**, 289 (2005).  
<sup>22</sup>V. A. Khodel, J. W. Clark, and M. V. Zverev, Europhys. Lett. **72**, 256 (2005).  
<sup>23</sup>K. Vakili, Y. P. Shkolnikov, E. Tutuc, E. P. De Poortere, and M. Shayegan, Phys. Rev. Lett. **92**, 226401 (2004).  
<sup>24</sup>Y. W. Tan, J. Zhu, H. L. Stormer, L. N. Pfeiffer, K. W. Baldwin, and K. W. West, Phys. Rev. Lett. **94**, 016405 (2005).  
<sup>25</sup>The variation of the extracted  $m$  in different samples and different cool-down conditions, found in Ref. 23, was attributed to sample inhomogeneities, as manifested by the spikes in the dependence of the electron mobility on  $n_s$ .  
<sup>26</sup>Y. Zhang and S. Das Sarma, Phys. Rev. B **72**, 075308 (2005).  
<sup>27</sup>R. Asgari and B. Tanatar, Phys. Rev. B **74**, 075301 (2006).